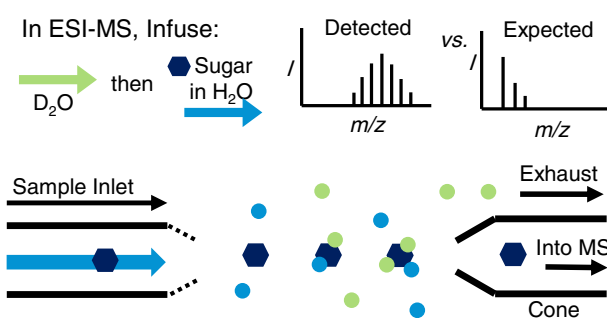


RESEARCH ARTICLE

Mass Spectral Detection of Forward- and Reverse-Hydrogen/Deuterium Exchange Resulting from Residual Solvent Vapors in Electrospray Sources

H. Jamie Kim, O. Tara Liyanage, Marina R. Mullenos, Elyssia S. Gallagher

Department of Chemistry and Biochemistry, Baylor University, One Bear Place #97348, Waco, TX 76798, USA



Abstract. Characterizing glycans is analytically challenging since glycans are heterogeneous, branched polymers with different three-dimensional conformations. Hydrogen/deuterium exchange-mass spectrometry (HDX-MS) has been used to analyze native conformations and dynamics of biomolecules by measuring the mass increase of analytes as labile protons are replaced with deuterium following exposure to deuterated solvents. The rate of exchange is dependent on

the chemical functional group, the presence of hydrogen bonds, pH, temperature, charge, and solvent accessibility. HDX-MS of carbohydrates is challenging due to the rapid exchange rate of hydroxyls. Here, we describe an observed HDX reaction associated with residual solvent vapors saturating electrospray sources. When undeuterated melezitose was infused after infusing D₂O, samples with up to 73% deuterium exchange were detected. This residual solvent HDX was observed for both carbohydrates and peptides in multiple instruments and dependent on sample infusion rate, infusion time, and deuterium content of the solvent. This residual solvent HDX was observed over several minutes of sample analysis and persisted long enough to alter the measured deuterium labeling and possibly change the interpretation of the results. This work illustrates that residual solvent HDX competes with in-solution HDX for rapidly exchanging functional groups. Thus, we propose conditions to minimize this effect, specifically for top-down, in-electrospray ionization, and quench-flow HDX experiments.

Keywords: Hydrogen/deuterium exchange, Mass spectrometry, Carbohydrates, Glycans, Peptides, Electrospray ionization

Received: 4 May 2018/Revised: 23 June 2018/Accepted: 23 June 2018/Published Online: 11 July 2018

Introduction

With estimates that over 50% of the human proteome is glycosylated [1], there is increased interest in characterizing the biological structures of glycans. Glycosylation is a post-translational modification where branched carbohydrates are attached to proteins. Glycans are synthesized by a non-template-driven process in which the final structure is

dependent on the enzymes that are present at the time of protein translation, producing heterogeneous structures with different monosaccharide composition, branching, and glycosidic bond stereochemistry. The complexity and diversity of glycans have multiple biological implications, including solubilizing and stabilizing folded proteins, and maintaining cellular communication and interactions, for instance to trigger immune responses [2]. Furthermore, glycans have shown promise as biomarkers for diseases, including cancer [3, 4] and a number of autoimmune diseases [5, 6]. For each of these systems, the three-dimensional structure of the glycan is crucial for glycoprotein function.

Hydrogen/deuterium exchange-mass spectrometry (HDX-MS) is a powerful technique for elucidating molecular

Electronic supplementary material The online version of this article (<https://doi.org/10.1007/s13361-018-2019-6>) contains supplementary material, which is available to authorized users.

Correspondence to: Elyssia Gallagher; e-mail: elyssia_gallagher@baylor.edu

structures, dynamics, and interactions. In HDX-MS, the mass increase of an analyte is measured as labile protons are replaced with deuterium (D) upon exposure to deuterated solvents. The rate of exchange is dependent on the chemical functional group, the presence of hydrogen bonds, pH, temperature, charge, and solvent accessibility [7, 8]. In traditional, bottom-up HDX procedures, proteins are diluted into D₂O-containing buffers for varying lengths of time. Following exchange, samples are quenched in acidic buffer (pH 2.5) to minimize back exchange, or loss of deuterium labels, at backbone amides. Pepsin or other acidic proteases are used to rapidly digest proteins and the resulting peptides are analyzed by liquid chromatography (LC)–MS. While quenching inhibits further deuterium labeling, back exchange occurs for rapidly exchanging side chains and some backbone amides [9] due to water in the quench buffer and solvents for proteolysis and LC [7]. Solution-phase HDX-MS of carbohydrates is challenging due to the rapid exchange rate of hydroxyls. Previous work by Guttman et al. [10] and Huang et al. [11] showed that amide-containing acetamido groups present in *N*-linked glycans retain deuterium in quench conditions and during sample work-up in bottom-up HDX-MS experiments. However, more rapidly exchanging functional groups, including hydroxyls, do not retain deuterium in quench conditions.

Other approaches to HDX can minimize back exchange, which may benefit HDX analysis of rapidly exchanging functional groups. Both bottom-up and top-down HDX-MS methods characterize analytes in their native, solvated conformations by exposing analytes to D₂O-containing buffers. However, top-down HDX eliminates in-solution sample work-up by ionizing immediately after quenching and using gas-phase fragmentation, rather than proteolytic digestion, to generate sub-local information [12]. Back exchange is significantly reduced for backbone amides through top-down HDX compared to bottom-up methods due to the shortened exposure time to protonated solvent, specifically quench buffer [12, 13]. Yet, there are several disadvantages to top-down proteomics, including extensive sample preparation to make biological samples suitable for MS analysis, lower sensitivity in MS compared to peptide analyses due to competing ionization of sample matrix components [14], and decreased signal-to-noise ratios associated with increasing molecular weight, often resulting in lower sequence coverage compared to that obtained for digested peptides [15]. Moreover, even the short exposure to acidic quench buffer in top-down HDX methods was found to alter protein conformations from the native structure that was present during protein labeling [16, 17], and thus, any forward or back exchange that occurred after quenching would sample the altered conformation.

Alternative HDX methods can be utilized to label rapidly exchanging functional groups with further reductions in back exchange. For gas-phase HDX, deuterating agents, such as ND₃ or D₂O, are introduced as gaseous vapors and interact with gas-phase analyte ions [18]. In-electrospray ionization (ESI) HDX methods involve exposing analytes to an atmosphere of gaseous D₂O in the source during droplet evaporation

and analyte ionization. Kostyukevich et al. described a method in which a droplet of D₂O was placed inside the instrument source, which vaporized in the heated environment, causing the analyte to come in contact with D₂O vapors during ionization [19]. Other in-ESI HDX methods introduce D₂O with the curtain gas [20, 21], nebulizer gas [21], through a dual sprayer [22], or through a GC-ESI interface [23, 24]. Both gas-phase HDX and in-source HDX with matrix assisted laser desorption ionization (MALDI) or ESI have been used to label carbohydrate hydroxyls [25–28]. These methods do not require quenching, thus minimizing back exchange. However, native conformations of carbohydrates may not be conserved as gas-phase ions during gas-phase HDX and at the end of the electrospray process. Strong inter-ring hydrogen bonding has been observed for carbohydrates in the gas-phase, whereas carbohydrates in solution exhibited more flexible conformations [29]. Therefore, analyses to characterize biologically active carbohydrates should examine solvated structures to maintain native conformations.

While new, in-ESI HDX methods can be utilized for analyzing carbohydrate hydroxyls by sampling short labeling times and preserving some solution-phase conformations. However, we present here a caveat to consider: the vapor composition and equilibrium in the ionization source is constantly modified by the residual and currently incoming solvent introduced by the sample inlet. Here, we show that the residual solvent vapors that accumulate inside the source affect deuterium labeling of rapidly exchanging functional groups, including hydroxyls. Although back exchange from the atmospheric environment has been reported before [30, 31], effects of residual solvents on deuterium labeling or back exchange of rapidly exchanging functional groups have not been studied. Our findings are distinguished from those methods that utilize solvent vapors for labeling, such as in-ESI HDX, because residual solvent vapors introduced from the current or previous runs, including blanks, are not controlled, can vary with time, and are often neglected between runs.

Further development of HDX methods for analysis of solvated, biologically active conformations of carbohydrates requires an understanding of the forward and back exchange that occurs between in-solution labeling and detection. Moreover, we show that residual solvent vapors affect deuterium exchange in multiple instruments for rapidly exchanging functional groups on other biomolecules, including peptides. This indicates that this effect extends beyond carbohydrates and may need to be taken into consideration as HDX continues to be developed and used for top-down and in-ESI methods.

Experimental

Materials

Melezitose, tri-*N*-acetylglucosamine (NAG₃), and sodium chloride (NaCl) were purchased from Sigma-Aldrich (St. Louis, MO). Deuterated solvents with purity > 99% (e.g., D₂O and CH₃OD, referred to as MeOD hereafter) were

purchased from Cambridge Isotope Laboratories, Inc. (Tewksbury, MA). [Glu1]-Fibrinopeptide B (EGVNDNEEGFFSAR, glu-fib) was purchased from Waters Corporation (Milford, MA). All other materials were purchased from Fisher Scientific International, Inc. (Pittsburgh, PA). All chemicals were used without further purification. Nanopure water was acquired from a Purelab Flex 3 purification system (Elga, Veolia Environnement S.A., Paris, France).

Sample Preparation

Carbohydrates were prepared with NaCl at a 1:10 M ratio in H₂O or D₂O to aid ionization by sodium adduction. This molar ratio, which gave the best signal for our experiments, was maintained for all experiments. Glu-fib was prepared in a 50:50 volumetric mixture of H₂O and acetonitrile with 0.2% formic acid.

HDX During Direct Infusion of Carbohydrates

Melezitose and NaCl were diluted into 99.9% D₂O (v/v) and immediately infused at 5, 10, or 20 μ L/min into a Waters Synapt G2-S High Definition MS (HDMS) with LockSpray Exact Mass Ionization Source (Waters Corporation, Milford, MA). Deuterium exchange was measured as melezitose was exposed to D₂O solvent for increasing lengths of time. Capillary voltage, source temperature, desolvation temperature, and desolvation gas flow rate were 2.5 kV, 100 °C, 350 °C, and 500 L/h, respectively. The syringe, capillary, and ESI needle were washed with nanopure water for at least 5 min between runs to prevent salt precipitation.

HDX Following Pre-Equilibration of the Source

Melezitose and NaCl were diluted in H₂O or D₂O and directly infused. In separate experiments, glu-fib was directly infused. Experiments were performed on the Waters Synapt G2-S HDMS with the conditions described above or an LTQ Orbitrap Discovery MS equipped with an Ion Max Source (Thermo-Fisher, Waltham, MA). For the Orbitrap instrument, the source voltage and capillary temperature were 4.5 kV and 250 °C to yield optimum ionization.

Each experiment was composed of three parts: pre-equilibration of the source, sample infusion, and source evacuation. The source was pre-equilibrated with solvent vapor by infusing solvent (D₂O, MeOD, H₂O, MeOH, or acetonitrile) for 5 min at 20 μ L/min. Then, the sample was infused at 10 μ L/min for 2 min (Synapt G2-S) or 5 min (Orbitrap Discovery). Unless stated otherwise, the sample was prepared in a solvent different from that used for pre-equilibration to test whether the observed HDX came from residual vapors. For instance, when the source was pre-equilibrated with a deuterating agent, undeuterated sample was infused; when the source was pre-equilibrated with protonated solvent, deuterated sample was characterized. Deuterated samples were prepared by incubating carbohydrates with NaCl in 99.9% D₂O for more than 48 h at

room temperature. This deuteration time effectively labeled all labile hydrogens, e.g., hydroxyls and amides, resulting in 11D for the carbohydrates, and this state (11D) will be referred to as “fully deuterated” in the rest of the text. Separate syringes and capillaries were used for samples in H₂O and samples in D₂O to minimize carryover of solvents and potential exchange reactions before ionization, introducing approximately 30 s between pre-equilibration and sample infusion. Each run was followed by 20 min of source evacuation with no solvent or sample infusion to re-equilibrate the source to atmospheric conditions and remove solvent vapors. All gas parameters were maintained at constant flow rates during pre-equilibration, sample infusion, and source evacuation, unless specified otherwise.

For each trial, deuterium exchange was plotted as a function of time. The time points on all plots represent the elapsed time starting from initial signal detection, with $t=0$ s as the first signal intensity above 500 ion counts with $S/N > 3$ for sodiated-carbohydrates.

HDX with Defined Solution Labeling Times

A mixing apparatus, modified from that described by Keppel et al. [32], was used to ensure that in-solution labeling times were strictly defined. Two syringes, attached to fused silica capillaries (150 μ m i.d., Polymicro Technologies, Phoenix, AZ), were joined to a mixing tee with a single outlet that connected to the ESI source. A 500- μ L syringe was filled with carbohydrates and NaCl in H₂O with 0.1% formic acid and a 2.5-mL syringe was filled with D₂O with 0.1% formic acid. Both syringes were pumped using a single syringe pump (Fusion 400, Chemyx, Inc. Stafford, TX), resulting in solution mixing for a specified length of time downstream of the mixing tee. The concentrations of carbohydrates and NaCl after dilution into D₂O were 5 and 50 μ M, respectively. Labeling time (t_{label}) was defined by Eq. (1).

$$t_{\text{label}} = \frac{V_d}{F_1 + F_2} \cdot l \quad (1)$$

F_1 and F_2 are the flow rates of each syringe, V_d is the volume of the delay line between the mixing tee and ESI source, and l is the length of the delay line. The flow rate through the labeling capillary was 18 μ L/min. The delay line included a capillary (150 μ m i.d. and 7 cm length) and the ESI needle (127 μ m i.d. and 23.57 cm length), resulting in a mixing time of 14.1 s.

Carbohydrates and NaCl mixtures were infused from the mixing apparatus for 5 min and the ESI needle was washed with H₂O containing 0.1% formic acid for 5 min. The source was not pre-equilibrated with solvent between runs but was evacuated for 45 min after each run, as described above for the pre-equilibration experiments. To prevent salt precipitation, the mixing tee was sonicated for 30 min in nanopure water during source evacuation.

Calculations

The theoretical, average masses of undeuterated (0D) and fully deuterated (11D) sodiated-carbohydrates (Figure S-1) were calculated using isotopic distributions generated by Exact Mass Calculator (IonSpec Corporation, now Varian, Inc., Palo Alto, CA) at a resolution of 20,000 (Eq. (2)), where m/z is the mass-to-charge ratio and I is the intensity of each peak. Exact masses are presented in Table 1.

$$(m/z) = \frac{\sum (m/z) \cdot I}{\sum I} \quad (2)$$

The average mass of experimentally observed sodiated-carbohydrates was calculated using each peak in collected mass spectra. Deuterium exchange (#D) and percent deuteration (%D) were calculated using Eqs. (3) and (4), respectively.

$$\#D = (m/z)_{\text{experimental}} - (m/z)_{\text{theoretical,0D}} \quad (3)$$

$$\%D = \frac{(m/z)_{\text{experimental}} - (m/z)_{\text{theoretical,0D}}}{(m/z)_{\text{theoretical,11D}} - (m/z)_{\text{theoretical,0D}}} \times 100 \quad (4)$$

LockMass was not used, as the lockspray standard was deuterated in the source during analysis (Figure 6).

Each experiment was repeated with a minimum of three replicates. Data figures plot average values with error bars representing standard deviations unless specified otherwise. Where necessary, statistical analyses utilized Student's t test at the 95% confidence interval.

Results and Discussion

Faster Sample Infusion Rates Increase the Deuterium Labeling Rate of Hydroxyls

Melezitose and NaCl were diluted into D₂O, loaded into a syringe, and immediately infused into the ESI source at 5 $\mu\text{L}/$

min to monitor in-solution exchange of hydroxyls. For this experiment, the labeling time increased as melezitose was incubated in the syringe with D₂O; thus, longer labeling times were achieved at later infusion times. Whereas the exchange rate of hydroxyls was expected to be on the microsecond time scale [33, 34], deuterium labeling was observed over 5 min (Figure 1). Back exchange from moisture in the atmosphere likely contributed to low deuterium labeling at the earliest time points, but the 5-min time frame that was required to observe exchange suggested that back exchange inside the source was greater than expected.

To improve the consistency of the spray and signal intensity at earlier time points (< 75 s), the flow rate was increased to 10 or 20 $\mu\text{L}/\text{min}$. Higher levels of deuterium labeling were measured with faster infusion rates at earlier time points (Figure 2). For instance, when infused at 10 $\mu\text{L}/\text{min}$, melezitose was only $24 \pm 7\%$ deuterated (2.7 ± 0.8 D) after 1 min of labeling, but when infused at 20 $\mu\text{L}/\text{min}$, melezitose reached $76 \pm 10\%$ deuteration (8 ± 1 D) even though the solution labeling time remained 1 min (Figure 2a). After 2 min of in-solution labeling, melezitose infused at 10 $\mu\text{L}/\text{min}$ or 20 $\mu\text{L}/\text{min}$ was $84 \pm 2\%$ (9.3 ± 0.2 D) or $88 \pm 2\%$ (9.8 ± 0.3 D) deuterated, respectively, whereas melezitose infused at 5 $\mu\text{L}/\text{min}$ was $55 \pm 12\%$ (6 ± 1 D) deuterated (Figure 2b). This observation is different from previously reported in-ESI HDX experiments in which the amount of deuterium labeling was described as independent of sample infusion rate [19].

Even though melezitose spent the same length of time interacting with the deuterating agent in solution, different deuterium exchange was measured when melezitose was infused at different flow rates, suggesting that an additional source of HDX was occurring as the carbohydrates were infused. Furthermore, when the source was pre-equilibrated with mixtures of D₂O and H₂O that matched the solvent composition of the sample, no difference in deuterium exchange was observed at varying flow rates or for different infusion times (Figure S-2). We hypothesized that D₂O vapors introduced along with the analyte were accumulating in the ESI source at a time scale long enough to promote in-ESI HDX of hydroxyls. For instance, when D₂O was infused at a faster flow rate, more

Table 1. Exact Mass-to-Charge Ratios (m/z) of Undeuterated (0D) and Fully Deuterated (11D) [Melezitose-Na]⁺ or [NAG₃-Na]⁺ with Isotopic Distributions

Peaks ^a	Melezitose			NAG ₃		
	m/z		Relative abundance	m/z		Relative abundance
	0D	11D		0D	11D	
M ₁	527.1588	538.2278	100.00	650.2385	661.3075	100.00
M ₂	528.1622	539.2312	20.44	651.2417	662.3107	28.00
M ₃	529.1640	540.2330	5.23	652.2438	663.3128	7.04
M ₄	530.1669	541.2359	0.79	653.2464	664.3154	1.24
M ₅				654.2487	665.3177	0.19
Average ^b	527.4227	538.4901		650.5807	661.6497	

^aPeaks correlate to isotopic distributions that are combinations of different numbers of naturally occurring ¹³C, ¹⁷O, and ¹⁵N that can be resolved at the given resolution of 20,000

^bThis is the weighted average of m/z values that were used for calculations of deuterium exchange

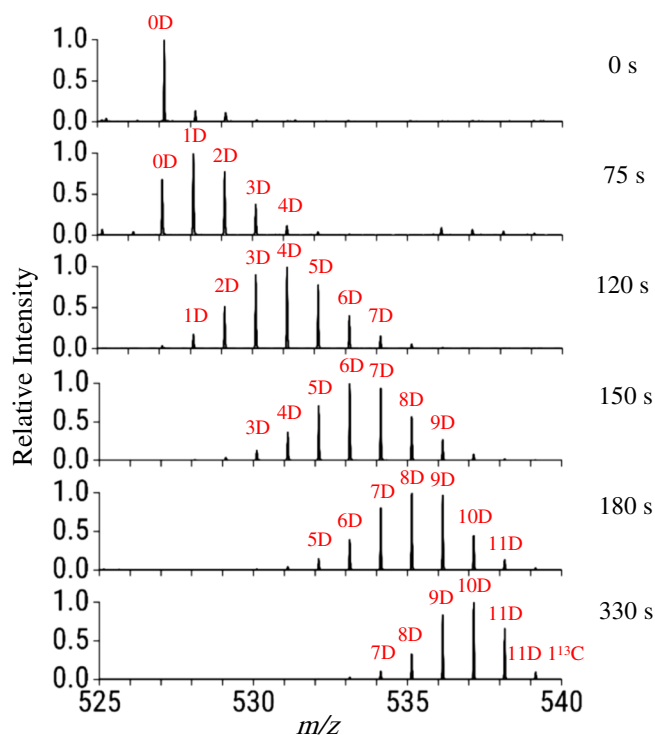


Figure 1. Representative deuterium-exchange spectra for sodiated-melezitose detected by ESI-MS. Melezitose and NaCl were diluted into D₂O (final solution 99% D₂O (v/v)) and spectra were collected at increasing solution incubation times

D₂O vapors accumulated in the source, resulting in more HDX in the same length of time. Alternatively, before D₂O vapors

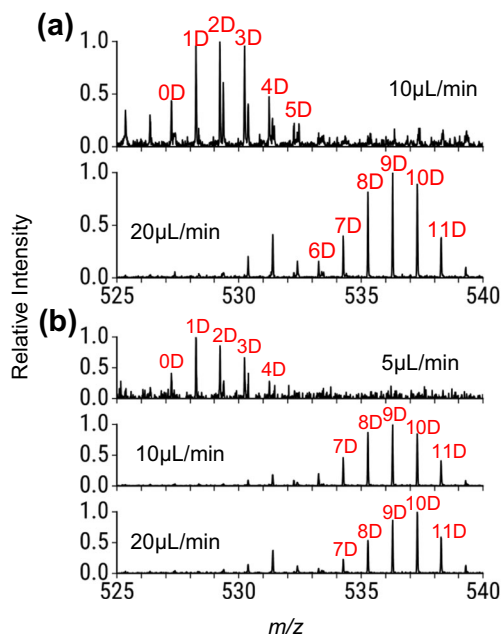


Figure 2. Representative HDX spectra for sodiated-melezitose infused at different rates. With a constant in-solution labeling time, (a) 1 min or (b) 2 min, deuterium labeling increased with faster sample infusion rates, indicating that an additional HDX labeling reaction was occurring besides the in-solution reaction

accumulated to an appreciable extent, atmospheric water vapor likely caused back exchange of the sample. Several assumptions were made in generating this hypothesis. First, we assumed that there was no additional exchange in the instrument under vacuum. Second, we assumed that the electrospray droplets desolvate in the source on the order of microseconds [35, 36], which correlates to the expected rate of hydroxyl exchange.

Residual Solvent Vapors in the ESI Source Result in HDX of Hydroxyls

To determine if residual vapors in the source were causing in-ESI HDX, the source was pre-equilibrated with D₂O, then protonated melezitose and NaCl in H₂O were directly infused. Although the carbohydrates were undeuterated, melezitose was detected at the earliest time point with an average of 8.0 ± 0.2 D, corresponding to $73 \pm 2\%$ deuteration (Figure 3a). The percent deuterium exchange decreased over time (Figure 3a, c). Because fully protonated melezitose was infused into the instrument, the deuterium exchange was attributed to HDX from residual solvent in the source. From the observation that deuterium labels were lost over time, it could be inferred that either the residual D₂O was evacuated at later time points or H-for-H exchange became greater than HDX at later time points due to increasing H₂O vapor as protonated solvent was infused.

Pre-equilibration with MeOD followed by infusion of undeuterated melezitose and NaCl also showed an initial deuterium exchange (Figure 3b). However, the initial deuterium exchange was considerably lower than that measured when pre-equilibrating with D₂O for the same length of time, with 0.4 ± 0.1 D ($3 \pm 1\%$). Though the average deuterium exchange was low, it was significantly higher than the average deuterium exchange measured after infusing the sample for 60 s (0.03 ± 0.01 D or $0.3 \pm 0.1\%$), indicating that residual MeOD vapors also caused HDX. When the source was pre-equilibrated with acetonitrile, which contains no labile hydrogens, and fully deuterated melezitose with NaCl was infused, residual acetonitrile resulted in no detected back exchange (Figure S-3). When the source was pre-equilibrated with H₂O or MeOH, fully deuterated melezitose showed back exchange at initial time points, with H₂O resulting in greater initial loss of deuterium than MeOH (Figure S-3), consistent with the data presented in Figure 3. Finally, when the source was pre-equilibrated with D₂O first, followed by an equal volume of acetonitrile, deuterium labeling from residual D₂O reduced to approximately 22% but was not completely removed (unpublished data). Based on the density of D₂O and MeOD, there are twice as many D₂O molecules as MeOD molecules in an equivalent volume of solvent. Also, D₂O has two deuteriums available for exchange whereas MeOD has only one. Therefore, pre-equilibration with D₂O results in four times as many deuterium present for labeling compared to MeOD pre-equilibration. However, initial deuterium exchange observed from

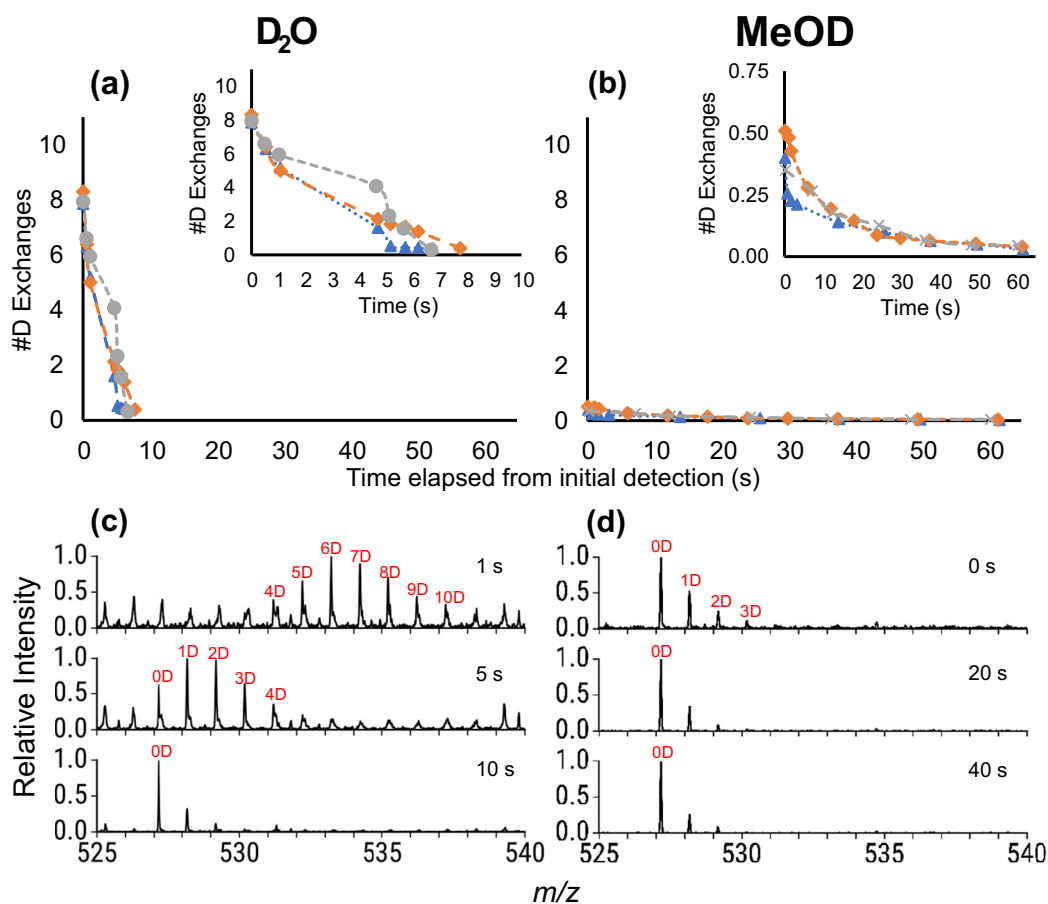


Figure 3. Residual solvent vapors caused in-ESI HDX of sodiated-melezitose. Deuterium exchange by melezitose is plotted for each replicate after pre-equilibration of the source with (a) D_2O or (b) MeOD. Different colors represent replicate experiments. Insets show expanded views of the time or deuterium exchange axes. (c) and (d) illustrate representative mass spectra of sodiated-melezitose at three-time points after pre-equilibration with D_2O or MeOD, respectively. Unlabeled peaks in the mass spectra are chemical noise and not used for deuterium exchange calculations

residual D_2O is still disproportionately larger than labeling from residual MeOD.

Several additional explanations are plausible for the difference in exchange between D_2O and MeOD. (1) Although higher levels of deuteration may have been achieved by melezitose from MeOD vapors, melezitose with higher deuterium labeling may not have been detected at these initial time points due to weak instrument signal. Thus, the first detected carbohydrates may have been exposed to a mixture of MeOD and H_2O vapors, resulting in less overall deuterium exchange. This point is supported by the observation that differences in spray stability within each run yielded different levels of initial deuterium labeling for each replicate. Additionally, data collected on a different instrument showed that higher levels of deuterium exchange could be observed from residual MeOD vapors (Figure 4). Or (2) MeOD was evacuated from the source faster than D_2O , resulting in a lower accumulation of MeOD vapors and less exchange. The difference in evacuation rates could be due to differences in the solvent volatilities and/or condensation coefficients on the surfaces of the ESI source [37]. The source temperature was varied to examine the effect of volatility and condensation coefficient on residual solvent

vapor HDX, but no observable correlation or statistical differences were found (Tables S-1 and S-2 and Figure S-4). Though increasing the temperature was expected to decrease HDX by increasing evacuation of the volatile solvents from the source, it

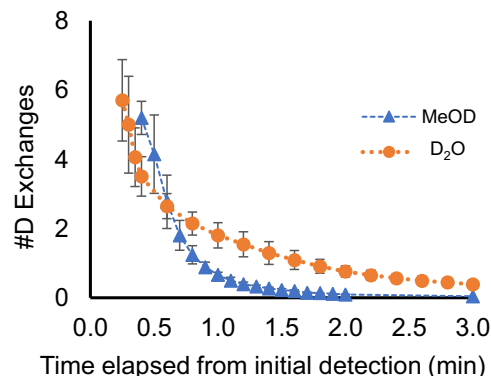


Figure 4. Residual solvent vapors were observed to cause HDX of sodiated-melezitose in an Ion Max Source of an LTQ Orbitrap Discovery MS. Deuterium exchange by sodiated-melezitose is plotted after pre-equilibration of the source with D_2O or MeOD

would also increase the rate of the exchange reaction according to the Arrhenius equation. By approximating the activation energy as between 2 and 10 kcal/mol for proton exchange between ethanol and water [38], an increase in temperature from 120 to 350 °C would result in a rate increase between 3 and 113 times faster. If the activation energy was approximated to be similar to that reported for exchange of backbone amide hydrogens [39, 40], the rate difference would increase by three to four orders of magnitude for these two temperatures. While an increase in the reaction rate would increase deuterium labeling, the back exchange rate would also increase at the higher temperature; thus, multiple forward and back exchanges could occur in the source prior to detection. In summary, all factors described above could contribute to the reduced deuterium exchange that was observed following MeOD pre-equilibration.

Guttman et al. identified a source of HDX specific to instruments with StepWave ion guides [41], including the Waters Synapt G2-S that was used to collect this data. StepWave ion guides consist of two stages where a DC offset potential is used to push ions from the lower stage to the higher stage leading into the mass spectrometer, while neutral, bulk species are retained in the lower stage [42]. It was hypothesized by Guttman et al. that residual bulk solvent may linger in the lower stage of the StepWave and exchange with analytes [41]. To verify that the labeling in our specific experiments occurred in the source and not the ion optics, we replicated our experiments in a Thermo LTQ Orbitrap Discovery with an Ion Max Source, which is equipped with a linear stacked ring ion guide. When undeuterated melezitose in H₂O was infused into the Ion Max source following pre-equilibration with D₂O or MeOD, deuterated melezitose was detected (Figure 4). For instance, when the source was pre-equilibrated with D₂O, melezitose with an average of 6 ± 1 D ($52 \pm 11\%$) was initially detected and the deuteration level decreased to 0.4 ± 0.1 D ($4 \pm 1\%$) at 3 min into the sample infusion. When the source was pre-equilibrated with MeOD, melezitose with 5.2 ± 0.5 D ($47 \pm 4\%$) was initially detected and was back exchanged to 0.12 ± 0.00 D ($1.08 \pm 0.01\%$ D) after 2 min of sample infusion. Because deuterated melezitose was observed following pre-equilibration of the source with deuterating agent, in an instrument with a different ion guide compared to that with a StepWave, it was concluded that the labeling was occurring in the source rather than the ion guide. Moreover, from earlier findings that sodium-adducted carbohydrates and other molecules display limited HDX in the gas-phase [25, 43–46], vaporized sodiated-melezitose adducts in ion guides are less likely to be labeled, unlike peptides and proteins. Thus, the data supports our hypothesis that exchange occurred in the source while the carbohydrates were partially solvated rather than as gas-phase ions in the ion guide optics.

An interesting observation is that while the level of deuteration decreased to < 0.5 D within 10 s in the Synapt G2-S, in the Orbitrap Discovery, melezitose maintained higher levels of deuteration for over 2 min, suggesting that the rate of source evacuation was higher for the Synapt G2-S, possibly due to the

faster build-up of pressure in the LockSpray Exact Mass Ionization Source. We hypothesized that changing the gas flow rates in the gas-tight ionization chamber of the LockSpray Exact Mass Ionization Source would alter the rate of evacuation of solvent vapors and the deuterium exchange of the sample; however, no apparent correlations were found with different gas flow rates (cone gas, desolvation gas, and nebulizer gas) and the residual solvent HDX (Table S-3 and Figure S-5). However, large variations between replicates suggested that ionization efficiency and spray stability could have affected the measurement of deuterium exchange as the gas flow rates were modified.

Solvent Vapors Differentially Affect Functional Groups with Different Exchange Rates

The deuterium exchange of melezitose and NAG₃ was compared to examine the effect of residual solvent vapor HDX on exchange of different functional groups (Figure S-1). The proton exchange rates of carbohydrate hydroxyls and acetamido hydrogens were assumed to be similar to those measured for serine hydroxyls and protein backbone amides, respectively. Thus, the difference in exchange rates was maximized at pH 2.5, where the exchange rate of hydroxyls was approximated to be eight orders of magnitude greater than that of backbone amides [47]. A mixing apparatus was used to define the in-solution labeling time to ensure that both melezitose and NAG₃ were exposed to D₂O_(l) solvent for the same length of time.

Even with the defined labeling time in solution, changes in deuterium labeling were observed for melezitose during the course of the experiment, confirming that HDX was occurring in the source. The average deuterium exchange for melezitose at the earliest time point was 10.78 ± 0.05 D ($97.4 \pm 0.5\%$) which decreased to 10.2 ± 0.4 D ($92 \pm 3\%$) after 1 min. The average deuterium exchange for NAG₃ was 8.8 ± 0.1 D ($78 \pm 1\%$) initially and 8.59 ± 0.05 D ($77.0 \pm 0.5\%$) near the end of the 5-min infusion. The decrease in deuterium exchange for melezitose was significant, implying that back exchange was occurring, likely from atmospheric water vapor in the source. Yet, the deuterium exchange for NAG₃ was consistent throughout the 5-min duration. This consistent level of deuterium labeling for NAG₃ illustrates, for the first time, that solvent vapors saturate the source during ESI. Despite the decrease in deuterium exchange, melezitose achieved a higher level of deuteration compared to NAG₃ (Figures 5 and S-6). This was expected due to the greater number of hydroxyls in melezitose.

The numerical values for deuterium exchange are quite interesting, considering that the D₂O:H₂O ratio was 5:1 or 83.33% D₂O by volume. When the source was pre-equilibrated with solvent mixtures matching the sample composition, the percent deuterium exchange was consistent with the percent deuterium of the solvent (Figure S-2). On the other hand, the deuteration level for neither melezitose nor NAG₃ matched the percentage of D₂O in solution (Figure 5), which would correspond to 9.17 D. The solvent pre-equilibration

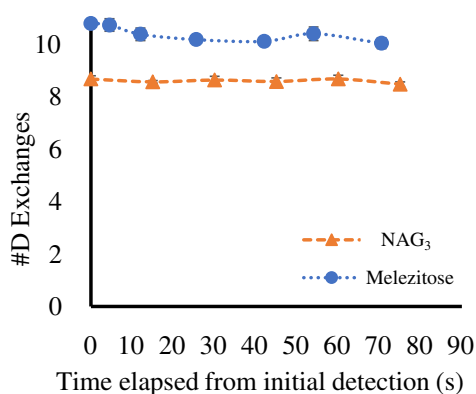


Figure 5. Deuterium exchange for sodiated-melezitose and sodiated-NAG₃ after a defined in-solution HDX time

experiments (Figure S-2) were performed without adjusting the solution pH; therefore, the exchange reaction was at neutral conditions. Because the exchange rate of hydroxyls is minimized around pH 6, at higher pH, e.g., neutral conditions, the exchange reaction is primarily catalyzed by OH⁻ or OD⁻ [7], whereas the experiments comparing deuterium exchange for melezitose and NAG₃ were performed at pH 2.5 and acid catalyzed. In changing the pH from neutral to 2.5, the exchange rate of hydroxyls would increase by approximately two orders of magnitude, while the exchange rate of amides would decrease by approximately five orders of magnitude [47]. For hydroxyls at pH 2.5, it would be expected that the forward labeling and back exchange rates would increase to an equal extent. Thus, though the exchange rate was faster at pH 2.5, it would equally affect the forward and back exchange reactions in solution and the source. Compared to the solvent pre-equilibration experiments (Figure S-2), the only difference in exchange conditions was the reaction pH, which appeared to result in an equilibrium favoring the deuterium-labeled species for melezitose at pH 2.5.

NAG₃ is a reducing sugar with eight hydroxyls when the reducing end forms a six-membered ring, as drawn in Figure S-1, whereas melezitose is a non-reducing sugar. Because all 11 hydroxyls of melezitose were found to be deuterated to some extent in the current setup with the mixing apparatus, the differences in exchange rate between primary and secondary hydroxyls is assumed to be negligible. Therefore, based on the deuterium labeling equilibrium of melezitose, seven hydroxyls of NAG₃ that are not involved in mutarotation would be expected to be labeled. The mutarotation rate between α and β anomers of *N*-acetyl glucosamine was reported as $0.7 \pm 0.09 \times 10^{-3} \text{ s}^{-1}$ at pH 8.99 with a trend of decreasing rate with lower pH [48]. Thus, with a solution labeling time of 14.1 s, interconversion between the chain and ring forms is expected but more likely to be catalyzed by D⁺ compared to H⁺ due to the volumetric percentages of D₂O and H₂O in the solvent. Thus, interconversion would preferentially add deuterium either to the C5 oxygen as the ring opened into the chain form or at the α or β hydroxyl at C1 as the ring forms from the aldehyde, increasing the total deuterium content of the molecule at an

eighth hydroxyl (Figure S-7). The observed deuterium exchange was greater than the number of hydroxyls on NAG₃. At pH 2.5, the intrinsic chemical HDX rate for backbone amides is slowed compared to neutral pH [7] but is still dependent on factors such as solvent accessibility and hydrogen bonding. Assuming the exchange rate of acetamido hydrogens is similar to that of backbone amides, it is possible that some of the amide hydrogens exchanged, given the minimal structuring and hydrogen bonding associated with the carbohydrate [49].

Solvent Vapors Affect Exchange of Glu-Fib Peptides

The effect of solvent vapor HDX on peptides was examined using glu-fib, a common peptide standard in instruments with time-of-flight mass analyzers. The LockSpray Exact Mass Ionization Source is a dual-electrospray source and glu-fib was introduced through the lockspray inlet. When undeuterated glu-fib peptides were infused through the lockspray needle after pre-equilibration of the source with D₂O, glu-fib was found to be deuterated (4 ± 1 D) and the deuteration level decreased over time (0.6 ± 0.2 D) (Figure 6a). The deuteration of glu-fib from residual solvent vapors illustrates several important points. First, because glu-fib and D₂O were infused through two separate spray needles, the lockspray and sample

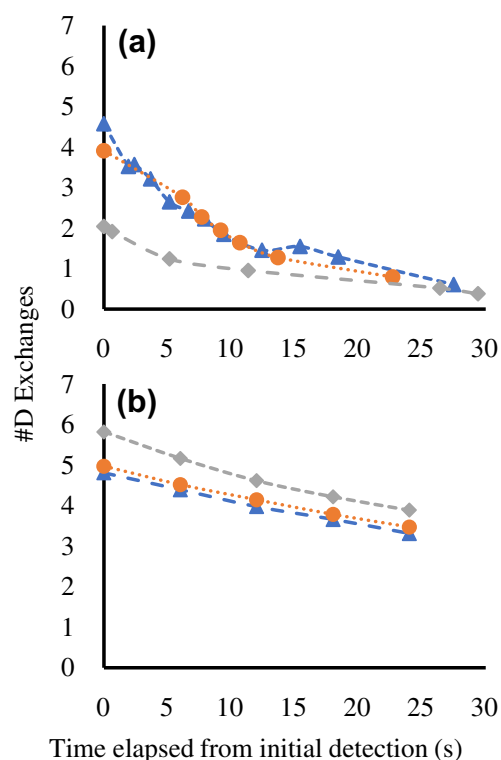


Figure 6. Residual solvent vapor HDX causes labeling of rapidly exchanging functional groups of glu-fib, a peptide. Deuterium exchange is plotted over time for glu-fib after pre-equilibration of the source with D₂O in (a) Waters Synapt G2-S HDMS with LockSpray Exact Mass Ionization Source or (b) Thermo LTQ Orbitrap Discovery MS with an Ion Max source. Different colors represent replicate experiments

spray, respectively, there was no dead volume, indicating that deuteration was a result of solvent vapor rather than residual solvent in a shared electrospray needle. Second, solvent vapor was found to exchange with peptide protons, suggesting that the residual solvent vapor HDX could affect peptide and protein analyses. Third, because glu-fib was deuterated by the residual solvent vapors, lockmass could not be used. For our experiments, the original undeuterated peptide mass could not be detected. Even if the undeuterated (0D) peak was detected, the presence of deuterated peaks would likely shift the m/z distribution and could cause incorrect lockmass assignment. A standard with no labile hydrogens would be required to use the lockmass function in the presence of deuterating vapors in the source.

Glu-fib was also characterized on the Thermo LTQ Orbitrap Discovery MS following source pre-equilibration with D_2O . A trend similar to the data from the Synapt G2-S was observed (Figure 6b). Glu-fib was initially detected with an average of 5.2 ± 0.5 D, and the deuteration level decreased to 0.84 ± 0.03 D by the end of the 5-min infusion time. The rate of decrease in deuteration was slower in the LTQ Orbitrap Discovery compared to that observed in the Synapt G2-S. After 30 s of data collection, the deuterium exchange in the Orbitrap Discovery decreased by 1.6 ± 0.3 D or $32 \pm 1.5\%$, compared to a decrease of 3 ± 1 D or $83 \pm 4\%$ for the Synapt G2-S. Because the observed glu-fib peptides are not sodiated, unlike the carbohydrates, the earlier observation from Guttman et al. describing the labeling effects from StepWaves [41] may have had an additive effect after residual solvent vapor HDX for experiments performed on the Synapt G2-S. The difference in deuterium exchange by glu-fib from two different instruments may be accounted for by the difference in the ion guide setup. However, since the effects of different ion guide optics parameters have been thoroughly studied by Guttman et al., no further optimizations to minimize deuterium exchange of glu-fib in the ion guides were performed.

Conclusion

Residual solvent vapors accumulate in electrospray sources and exchange with rapidly exchanging functional groups of carbohydrates and peptides. This effect is distinguished from previously reported back exchange from atmospheric moisture or in-ESI HDX techniques, in that the HDX reported here results from saturation of the source with solvent vapors during an ongoing experiment. Residual solvent vapor HDX was observed on two different instruments. The magnitude of this effect was dependent on the sample infusion rate and time as well as the deuterium content (v/v) of the solvent. Furthermore, as the vapor composition in the source changed with time, the observed deuterium exchange was altered. Since residual solvent vapor HDX occurs after in-solution labeling, non-native conformations could be sampled. Thus, the structure of the analyte should be considered during ionization and desolvation. Additionally, the residual solvent vapor HDX is

significant because it shows that many biomolecules, including carbohydrates and amino acid side chains of peptides and proteins, are affected by this phenomenon. Thus, any biomolecules with rapidly exchanging functional groups could be deuterium-labeled or back exchanged in electrospray sources, but many current methods for data analysis assume peptide labeling occurs at backbone amides. Thus, these results suggest that simple assumptions about deuterium-labeled sites in proteins should be carefully considered.

Through our experiments, we observed a number of ways to reduce the effects of residual solvent vapor HDX. Traditional bottom-up HDX methods that introduce peptides in protonated solvents into the source are unlikely to be affected by residual solvent vapor HDX. However, protocols that involve high percentages of labeling solvent and rapid quench times, combined with microliter per minute flow rates will be more susceptible to residual solvent vapor HDX. As additional top-down, in-ESI, or quench-flow HDX methods are developed, this residual solvent vapor exchange will need to be controlled and/or measured when the deuterating reagent is introduced into the source as a volumetric fraction of the solvent. For many in-ESI HDX experiments, the residual solvent vapors will need to be removed between runs. This can be achieved in the following ways. For all the data presented here, "evacuation," or 20-min purging with source gas and no solvent introduction was included to ensure removal of residual solvent vapors. Opening the source for the Orbitrap Discovery also effectively reset the source to atmospheric conditions. Furthermore, purging the source after equilibrating to atmosphere with aprotic solvent (e.g., acetonitrile) minimized back exchange associated with environmental water vapor. However, purging with aprotic solvent alone (without evacuating) was not sufficient to remove all residual solvent vapors in the source. Similarly, purging the source with dry air would also reduce back exchange from atmospheric moisture [30]. For many top-down and quench-flow HDX experiments, it may be more important to maintain the same deuterium content in the source as in solution. This could be done by first pre-equilibrating the source with a solvent consisting of the same percentage of deuterating and aqueous (quench) reagents as the samples that will be analyzed. Because many variables including instrument parameters, analyte, solvent, and source shape could affect the extent and pattern of residual solvent vapor HDX, we recommend that the undesired effects be tested prior to running a full HDX experiment to ensure minimal residual solvent vapor HDX.

Acknowledgements

This work was supported by the Welch Foundation, Grant AA-1899. The authors acknowledge the Baylor University Mass Spectrometry Center. The authors thank Amber Taylor for initial assessment of the mixing apparatus efficiency. HJK and ESG developed the experimental design. HJK, OTL, and MRM conducted experiments and analyzed data.

HJK and ESG wrote the draft and all authors approved the final manuscript.

References

- Apweiler, R., Hermjakob, H., Sharon, N.: On the frequency of protein glycosylation, as deduced from analysis of the SWISS-PROT database. *Biochim. Biophys. Acta Gen. Subj.* **1473**, 4–8 (1999)
- Varki, A., C., R., Esko, J.D., et al. (eds.): *Essentials of Glycobiology*, 3rd edn. Cold Spring Harbor Laboratory Press, Cold Spring Harbor (NY) (2015–2017) Available from: <https://www.ncbi.nlm.nih.gov/books/NBK310274/>
- Brockhausen, I.: Glycodynamics of mucin biosynthesis in gastrointestinal tumor cells. In: Axford, J.S. (ed.) *Glycobiology and Medicine*. 163–188, Springer US, Boston, MA (2003)
- Dube, D.H., Bertozzi, C.R.: Glycans in cancer and inflammation—potential for therapeutics and diagnostics. *Nat. Rev. Drug Discov.* **4**, 477 (2005)
- Saso, L., Silvestrini, B., Guglielmotti, A., Lahita, R., Cheng, C.Y.: Abnormal glycosylation of $\alpha 2$ -macroglobulin, a non-acute-phase protein, in patients with autoimmune diseases. *Inflammation*. **17**, 465–479 (1993)
- Tramontano, A., Makker, S.P.: Conformation and glycosylation of a megalin fragment correlate with nephritogenicity in Heymann nephritis. *J. Immunol.* **172**, 2367–2373 (2004)
- Gallagher, E.S., Hudgens, J.W.: Mapping protein–ligand interactions with proteolytic fragmentation, hydrogen/deuterium exchange-mass spectrometry. In: Kelman, Z. (ed.) *Methods Enzymol.* Vol. 566, 357–404, Academic Press, (2016)
- Shaw, B.F., Arthanari, H., Narovlyansky, M., Durazo, A., Frueh, D.P., Pollastri, M.P., Lee, A., Bilgicer, B., Gygi, S.P., Wagner, G., Whitesides, G.M.: Neutralizing positive charges at the surface of a protein lowers its rate of amide hydrogen exchange without altering its structure or increasing its thermostability. *J. Am. Chem. Soc.* **132**, 17411–17425 (2010)
- Bai, Y., Milne, J.S., Mayne, L., Englander, S.W.: Primary structure effects on peptide group hydrogen exchange. *Proteins: Structure, Function and Bioinformatics*. **17**, 75–86 (1993)
- Guttman, M., Scian, M., Lee, K.K.: Tracking hydrogen/deuterium exchange at glycan sites in glycoproteins by mass spectrometry. *Anal. Chem.* **83**, 7492–7499 (2011)
- Huang, R.Y.C., Hudgens, J.W.: Effects of desialylation on human $\alpha 1$ -acid glycoprotein–ligand interactions. *Biochemistry*. **52**, 7127–7136 (2013)
- Pan, J., Han, J., Borchers, C.H., Konermann, L.: Hydrogen/deuterium exchange mass spectrometry with top-down electron capture dissociation for characterizing structural transitions of a 17 kDa protein. *J. Am. Chem. Soc.* **131**, 12801–12808 (2009)
- Englander, S.W.: Hydrogen exchange and mass spectrometry: a historical perspective. *J. Am. Soc. Mass Spectrom.* **17**, 1481–1489 (2006)
- Chait, B.T.: Mass spectrometry: bottom-up or top-down? *Science*. **314**, 65–66 (2006)
- Compton, P.D., Zamdborg, L., Thomas, P.M., Kelleher, N.L.: On the scalability and requirements of whole protein mass spectrometry. *Anal. Chem.* **83**, 6868–6874 (2011)
- Shen, L.L., Hermans, J.: Kinetics of conformation change of sperm-whale myoglobin. I. Folding and unfolding of metmyoglobin following pH jump. *Biochemistry*. **11**, 1836–1841 (1972)
- Konermann, L., Rosell, F.I., Mauk, A.G., Douglas, D.J.: Acid-induced denaturation of myoglobin studied by time-resolved electrospray ionization mass spectrometry. *Biochemistry*. **36**, 6448–6454 (1997)
- Winger, B.E., Light-Wahl, K.J., Rockwood, A.L., Smith, R.D.: Probing qualitative conformation differences of multiply protonated gas-phase proteins via hydrogen/deuterium isotopic exchange with water-d₂. *J. Am. Chem. Soc.* **114**, 5897–5898 (1992)
- Kostyukevich, Y., Kononikhin, A., Popov, I., Nikolaev, E.: Simple atmospheric hydrogen/deuterium exchange method for enumeration of labile hydrogens by electrospray ionization mass spectrometry. *Anal. Chem.* **85**, 5330–5334 (2013)
- Takáts, Z., Schlosser, G., Vékey, K.: Hydrogen/deuterium exchange of electrosprayed ions in the atmospheric interface of a commercial triple-quadrupole mass spectrometer. *Int. J. Mass Spectrom.* **228**, 729–741 (2003)
- Hemling, M.E., Conboy, J.J., Bean, M.F., Mentzer, M., Carr, S.A.: Gas phase hydrogen/deuterium exchange in electrospray ionization mass spectrometry as a practical tool for structure elucidation. *J. Am. Soc. Mass Spectrom.* **5**, 434–442 (1994)
- Wolff, J.-C., Laures, A.M.F.: ‘On-the-fly’ hydrogen/deuterium exchange liquid chromatography/mass spectrometry using a dual-sprayer atmospheric pressure ionisation source. *Rapid Commun. Mass Spectrom.* **20**, 3769–3779 (2006)
- Jeong, E.S., Cha, E., Cha, S., Kim, S., Oh, H.B., Kwon, O.-S., Lee, J.: Online simultaneous hydrogen/deuterium exchange of multitarget gas-phase molecules by electrospray ionization mass spectrometry coupled with gas chromatography. *Anal. Chem.* **89**, 12284–12292 (2017)
- Brenner, N., Haapala, M., Vuorensola, K., Kostianinen, R.: Simple coupling of gas chromatography to electrospray ionization mass spectrometry. *Anal. Chem.* **80**, 8334–8339 (2008)
- Uppal, S.S., Beasley, S.E., Scian, M., Guttman, M.: Gas-phase hydrogen/deuterium exchange for distinguishing isomeric carbohydrate ions. *Anal. Chem.* **89**, 4737–4742 (2017)
- Price, N.P.J.: Oligosaccharide structures studied by hydrogen–deuterium exchange and MALDI-TOF mass spectrometry. *Anal. Chem.* **78**, 5302–5308 (2006)
- Kostyukevich, Y., Kononikhin, A., Popov, I., Nikolaev, E.: In-ESI source hydrogen/deuterium exchange of carbohydrate ions. *Anal. Chem.* **86**, 2595–2600 (2014)
- Kostyukevich, Y., Kononikhin, A., Popov, I., Nikolaev, E.: Conformations of cationized linear oligosaccharides revealed by FTMS combined with in-ESI H/D exchange. *J. Mass Spectrom.* **50**, 1150–1156 (2015)
- Jockusch, R.A., Kroemer, R.T., Talbot, F.O., Snoek, L.C., Çarçabal, P., Simons, J.P., Havenith, M., Bakker, J.M., Compagnon, I., Meijer, G., von Helden, G.: Probing the glycosidic linkage: UV and IR ion-dip spectroscopy of a Lactoside. *J. Am. Chem. Soc.* **126**, 5709–5714 (2004)
- McCloskey, J.A.: Introduction of deuterium by exchange for measurement by mass spectrometry. In: McCloskey, J.A. (ed.) *Methods Enzymol.* Vol. 193, 329–338, Academic Press, (1990)
- Katta, V., Chait, B.T.: Hydrogen/deuterium exchange electrospray ionization mass spectrometry: a method for probing protein conformational changes in solution. *J. Am. Chem. Soc.* **115**, 6317–6321 (1993)
- Keppel, T.R., Weis, D.D.: Analysis of disordered proteins using a simple apparatus for millisecond quench-flow H/D exchange. *Anal. Chem.* **85**, 5161–5168 (2013)
- Englander, S.W., Downer, N.W., A., Teitelbaum, H.: Hydrogen exchange. *Annu. Rev. Biochem.* **41**, 903–924 (1972)
- Liepinsh, E., Otting, G.: Proton exchange rates from amino acid side chains—implications for image contrast. *Magn. Reson. Med.* **35**, 30–42 (1996)
- Mortensen, D.N., Williams, E.R.: Theta-glass capillaries in electrospray ionization: rapid mixing and short droplet lifetimes. *Anal. Chem.* **86**, 9315–9321 (2014)
- Smith, J.N., Flagan, R.C., Beauchamp, J.L.: Droplet evaporation and discharge dynamics in electrospray ionization. *J. Phys. Chem. A*. **106**, 9957–9967 (2002)
- Singh, B., Thomas, J.H. I: Chapter 1.8 - Surface physics and its relation to vacuum science. In: Hoffman, D.M., Singh, B., Thomas, J.H. I (eds.) *Handbook of Vacuum Science and Technology*, 40–55, Academic Press, San Diego (1998)
- Bureiko, S.F., Denisov, G.S., Lange, I.Y.: Kinetics of the fast proton exchange between ethanol and water in an inert solvent. *Kinet. Catal. (Engl. Transl.)* 1976, 17(6), 1232–1235. *Kinet. Catal.* **17**(6), 1431–1434 (1976)
- Klotz, I.M., Frank, B.H.: Activation energy of deuterium-hydrogen exchange in amides. *J. Am. Chem. Soc.* **86**, 3889–3889 (1964)
- Offenbacher, A.R., Iavarone, A.T., Klinman, J.P.: Hydrogen–deuterium exchange reveals long-range dynamical allostery in soybean lipoygenase. *J. Biol. Chem.* **293**, 1138–1148 (2018)
- Guttman, M., Wales, T.E., Whittington, D., Engen, J.R., Brown, J.M., Lee, K.K.: Tuning a high transmission ion guide to prevent gas-phase proton exchange during H/D exchange MS analysis. *J. Am. Soc. Mass Spectrom.* **27**, 662–668 (2016)
- Waters (2011). Dramatically enhanced analytical sensitivity with the use of novel StepWave ion transfer technology in the Synapt G2-S system (Application Note Literature No. 720003964EN). Waters, Milford, MA. Retrieved from <http://www.waters.com/webassets/cms/library/docs/720003964en.pdf>

43. Kaltashov, I.A., Doroshenko, V.M., Cotter, R.J.: Gas phase hydrogen/deuterium exchange reactions of peptide ions in a quadrupole ion trap mass spectrometer. *Proteins: Structure, Function and Bioinformatics*. **28**, 53–58 (1997)
44. Reyzer, M.L., Brodbelt, J.S.: Gas-phase H/D exchange reactions of polyamine complexes: (M + H)⁺, (M + alkali metal)⁺, and (M + 2H)²⁺. *J. Am. Soc. Mass Spectrom.* **11**, 711–721 (2000)
45. Jurchen, J.C., Cooper, R.E., Williams, E.R.: The role of acidic residues and of sodium ion adduction on the gas-phase H/D exchange of peptides and peptide dimers. *J. Am. Soc. Mass Spectrom.* **14**, 1477–1487 (2003)
46. Chen, Y., Yue, L., Li, Z., Ding, X., Wang, L., Dai, X., Fang, X., Pan, Y., Ding, C.-F.: Investigation of protonated and sodiated leucine-enkephalin by hydrogen-deuterium exchange and theoretical calculations. *Anal. Methods*. **7**, 5551–5556 (2015)
47. Dempsey, C.E.: Hydrogen exchange in peptides and proteins using NMR spectroscopy. *Prog. Nucl. Magn. Reson. Spectrosc.* **39**, 135–170 (2001)
48. Skelley, A.M., Mathies, R.A.: Rapid on-column analysis of glucosamine and its mutarotation by microchip capillary electrophoresis. *J. Chromatogr. A*. **1132**, 304–309 (2006)
49. Englander, S.W., Kallenbach, N.R.: Hydrogen exchange and structural dynamics of proteins and nucleic acids. *Q. Rev. Biophys.* **16**, 521–655 (1983)